Quantitative measures of comparison between antenna pattern data sets

J. McCormick, S.F. Gregson and C.G. Parini

Abstract: Frequently in test, measurement and development, there is a requirement to compare two or more supposedly identical data sets. These data sets may be acquired as: test data (does the data set fall within a given level of conformance); validation data (do the results confirm the applicability of a test methodology or design process); and calibration data (the data is required to act as a benchmark against which other measurements will be assessed). An example of such data is the far-field three-dimensional radiation pattern of antennas, which may be measured repeatedly on the same or different antenna test ranges. The requirement for objective, quantitative and robust methods of assessing such data, is discussed and confirmed. In addition, the constraints placed on these assessment methods, applied by the nature of the measurement process and the measurand, are highlighted and examined. Data sets that can be used to illustrate the application of these comparison techniques are presented and a preliminary assessment of them made using previously established techniques. These data sets embody a variety of subtle and specific characteristics that stem from particular known error sources. The limitations of these established assessment techniques are discussed and used to motivate the development of newer, more sophisticated analysis, where the data sets are further processed to yield objective measures of comparison. A variety of new assessment techniques that satisfy the aforementioned constraints are then presented and their various merits are compared and contrasted to illustrate their applicability to the classification and analysis of large data sets derived from near-field antenna measurements.

1 Introduction

Attempts to produce objective quantitative measures of comparison between data sets, that can be used to assess the accuracy, sensitivity and repeatability associated with the production of such antenna data has been widely reported [1–3].

The utility of such comparisons, or measures of adjacency between data sets, lies not only in their ability to determine the degree of similarity between various data sets but also in their ability to categorise the way in which these sets differ. Without the ability to produce such metrics of similarity any assessment as to the integrity of a data set is necessarily reduced to subjective value judgements.

A number of methods, some of which will be illustrated in this paper, have been developed in signal analysis to assess and quantify such differences. However, ongoing advances in antenna measurements and the nature of the data sets these advanced techniques produce requires the development of new and novel assessment techniques.

2 The nature of the measurand

A classical interpretation of antenna characteristics based on Maxwell's equations is a suitable mathematical algorithm in a large variety of different circumstances. However, the limitations imposed by this scheme, particularly with regard to the antinomy of the electron mass/energy and its implications for radiation resistance [4], mean that this interpretation of the action of antenna-to-antenna coupling can have limited applicability.

For antenna patterns a more fundamental physical interpretation, which concentrates on the irreversible macroscopic process of measurement, can be useful in assessing the process of radiative emission/absorption. The Schrodinger wave equation, the Dirac equation, or quantum electrodynamics (QED) can all be useful as conceptual models when attempting to assess data sets produced as a result of measuring antenna-to-antenna coupling. This is because they all are empirically based interpretations that concentrate on the process of measurement prediction as opposed to the mechanism of electromagnetic interaction.

In this paper, only Tx and Rx antennas that are in translational equilibrium will be considered and their velocities relative to each other will be specified to be zero. Additionally, the electromagnetic interactions will be observed from an inertial reference frame coincident with the fiducial mechanical datum of the Tx antenna. These conditions make it possible to consider the antenna characterisation without consideration of any relativistic effects associated with a multiplicity of reference frames or to any non-inertial effects. This simplifies the explanations, without invalidating them in more complex situations, and makes it possible to consider the measurement process in terms of non-relativistic wave mechanics.

Here, the antenna pattern is described by electron-photon-electron interactions that can only be specified by the probability of interaction, where this resultant

IEE Proceedings online no. 20045005

doi:10.1049/ip-map:20045005

Paper received 23rd April 2004

J. McCormick and S.F. Gregson are with the Sensor Systems Division, BAE Systems, Crewe Road North, Crewe Toll, Edinburgh, EH5 2XS, UK

C.G. Parini is with the Department of Electronic Engineering, Queen Mary, University of London, Mile End Road, London E1 4NS, UK

probability is formed by the superposition of complex probability amplitudes. Thus, the antenna pattern, that is classically considered as defining the relative power flux density propagating to or from an antenna, is more correctly described as the probability of discrete electron–photon–electron interactions. Here, the probability of interaction is given over known solid angles, relative to the antenna under test (AUT) placed at the centre of the inertial frame of reference. Consequently, the AUT pattern can be legitimately interpreted as a frequency distribution for these interactions that, when normalised to unity, can be recognised as an angular probability density function describing the process of electromagnetic interaction.

Previously, the comparison of such large data sets that can be recognised as probability density distributions has been significantly simplified by the techniques of statistical pattern recognition [2]. The application of statistical techniques is particularly appropriate to antenna patterns as stated above when the nature of the pattern is not constrained to the conventional classical interpretation, i.e. is not restricted to being considered as an angular spectrum of electromagnetic waves propagating in diverse directions.

Furthermore, the statistical approach has the inherent advantage that it can be used to consider the global, i.e. non-local, features of the data set and distils the complexity of the pattern into an alternative, dimensionally reduced, set of virtually unique features that can be utilised to describe the data. This extraction of global features is of particular relevance for antenna patterns as it takes account of the inherently anti-reductionist and holistic nature of the integral transforms that relate the aperture excitation to the angular far-field pattern. The holistic nature of the respective domains can be readily expounded, as a change in any part of the spatial domain will result in a corresponding change to every part of the spectral domain and *vice versa*.

3 Partial scans

To illustrate the applicability of these data assessment techniques to antenna measurements, a partial scan technique, which attempts to reduce truncation errors in near-field antenna measurements, will be simulated. This measurement technique occupies a research area that produces data sets that require detailed analysis to assess its applicability and utility as a measurement process. Moving the AUT between successive partial scans will necessarily involve the disturbance of the reference path of the RF subsystem and introduce further imperfections in the alignment between the antenna and the range. It is the impact of these imperfections that will be assessed.

In the absence of a detailed understanding of the uncertainties associated with this technique, a number of metrics have been produced to compare the results of this partial scan process to more conventional near-field antenna measurement techniques. A description of these partial scan techniques described in [5] and its development is not the purpose of this paper. However to illustrate the assessment processes a number of such simulated measurements with in-built errors were produced. These simulations were designed to replicate the degree of misalignment between adjacent scans that has been observed in practice. Figure 1 illustrates the particular tri-scan measurement process that is to be examined using the simulations.

Hitherto, the purpose of measurement simulations has been limited to the assessment of the relative merits of various transformation algorithms and measurement configurations. Here however, the simulation technique was

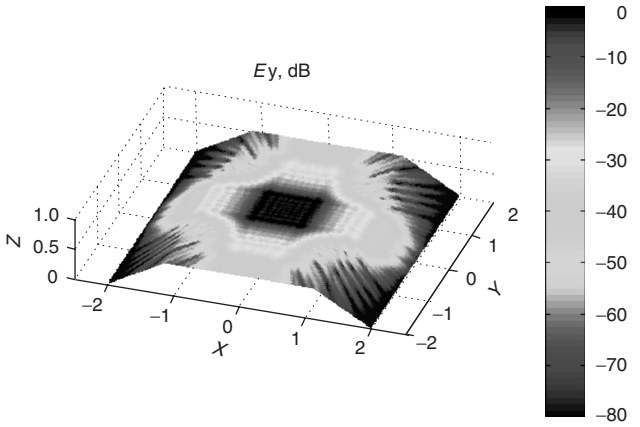

Fig. 1 *Pseudo-colour plot of simulated near-field power for tri-scan configuration*

utilised to produce a series of measurement simulations that could be used to yield a knowledge of the nature and magnitude of two alignment errors that were thought to be particularly pertinent to the auxiliary rotation partial scan technique under consideration.

4 Measurement error simulations and their conventional assessment

In the absence of some overriding definitive standard or infallible model, the only practical methodology for assessing the ability of any test facility to make measurements is by way of repetition of these measurements. This repetition can be accomplished without alteration in the measurement configuration, to simply address repeatability and precision, or with the inclusion of parametric variations to assess sensitivity. The parametric variations can also be used to assess the accuracy of the measurement if enough thought is devoted to the nature and extent of the parametric variations to be used, along with the types of analysis that are to be employed in the assessment process.

As, in the absence of systematic error in a measurement procedure, repeatability is itself inherently a statistical process [6], the validity of any conclusions drawn will greatly depend upon the size of the sample. Thus it is preferable in this case to utilise as large a number of simulations as is practical.

4.1 Simulation of partial scan plane pointing error

Simulation software was modified to enable the specification of angular and distance errors to partial scan configurations. The magnitude of the angular error introduced by the AUT positioner was estimated from observations of the variation in the boresight direction reported during active alignment correction verification measurements, and was of the order of $\pm 0.02^{\circ}$. These azimuth, elevation and roll errors were then used in the simulation of the acquisition planes.

The errors introduced into the alignment of the planes were based on uniformly distributed pseudo random numbers with a maximum range of plus or minus three times the standard deviation of the pointing error observed empirically. The use of a uniform distribution was though to be preferable to the more commonly employed normal distribution, as the former will inevitably produce a more pessimistic set of simulations. Thus 99 measurement

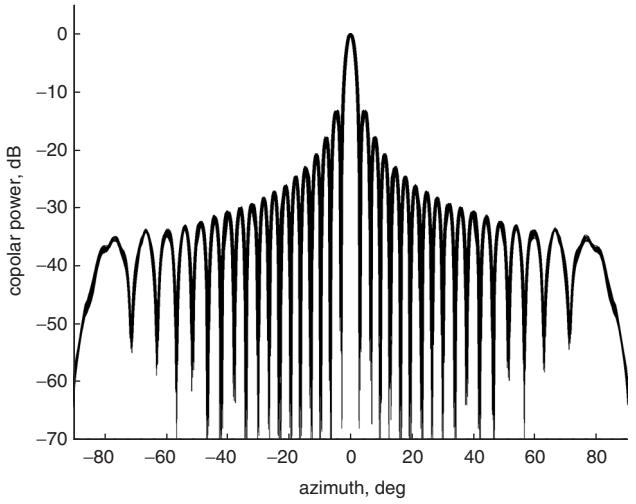

Fig. 2 *Far-field azimuth cut of error simulations*

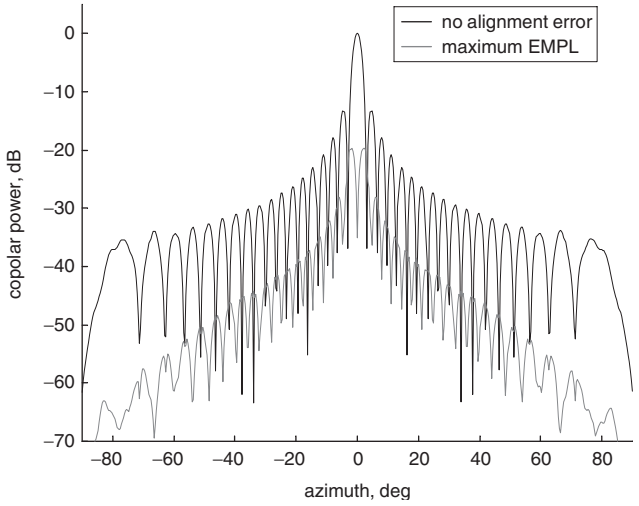

Fig. 3 *Far-field azimuth cut of ideal simulation and maximum EMPL*

simulations were produced all with different angular scan plane pointing errors.

The assessment of each of these errors entailed the simulation of the 99 tri-scan measurements, i.e. 297 individual partial planes. These measurement sets were transformed to the far field using existing transformation computer code assuming that the data sets contained no imperfections in their alignment. Figure 2 contains overlaid Ludwig III co-polar azimuth cardinal cuts from all of the transforms.

Clearly, the pointing errors introduce pattern measurement errors at all angles and at all levels in the far field. The equivalent multipath error (EMPL) was calculated between the ideal pattern and each of the error simulations. This can be thought of as the amplitude necessary to force the different pattern values to be equal. If no account is to be taken of the phase of the patterns, as is often the case when assessing far-field data, then the EMPL can be expressed in terms of the amplitude of the samples as

$$\text{EMPL}|_{dB} = 20\log_{10}\left(\frac{\| E_1(\theta,\phi)| - |E_2(\theta,\phi)\|}{2}\right) \quad (1)$$

Here, the factor of a half has been included as it is assumed that the 'correct' value lies between the two measured samples. The maximum EMPL, i.e. the worst case value at each angle can be found plotted in Fig. 3 together with the ideal cardinal cut.

The perfect alignment result plotted with the upper bound EMPL value at each angle from all 99 simulations shows that away from boresight, the EMPL seems to demonstrate a good degree of correlation and that the error term is proportional to the signal level. Although raising the maximum EMPL to perhaps as little as 20 dB below the error free signal, the auxiliary rotation system shows a degree of resilience to angular errors in the positioning of the partial scans and is sufficiently resilient to avoid a catastrophic break down. Thus, as its failure is gradual this illustrates a degree of robustness that should be observed in practice.

Other conventional measures of correspondence, not so closely associated with antenna measurements, can also be used to assess the alignment of the data sets. The peak signal to noise ratio (PSNR) is used to measure the difference between two data sets, where the elements have values that lie in the range $0 \leq |I(i)| \leq 1$. The PSNR is often given in decibel (dB) units, which can be used to measure the ratio of the peak signal, 1 V, and the difference

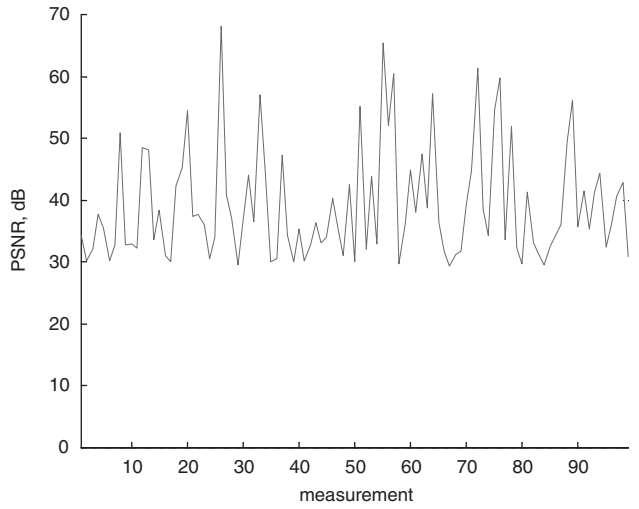

Fig. 4 *$PSNR_{dB}$ for 99 angular errors*

between two data sets $I_1(i)$ and $I_2(i)$, using the formula

$$\text{PSNR}|_{dB} = 20\log_{10}\left(\frac{1}{\sqrt{\frac{1}{N}\sum_{i-1}^{N}(I_i(i) - I_2(i))^2}}\right) \quad (2)$$

Clearly, when $I_1(i) = I_2(i)$, for all values of i the two data sets are identical, thus the PSNR in this case will be infinite. Although there are several different definitions for the signal-to-noise ratio, this choice is commonly employed for the purposes of digital image processing. For the simulated angular errors calculated above this produces the results summarised in Fig. 4.

Here, the calculations for the 99 cases have been displayed on the same plot and, for ease of observation, a solid line has been used to join the calculated values. If two signals, such as antenna patterns, vary similarly point for point then a measure of their similarity may also be obtained by taking the sum of the products of the corresponding pairs of points. If the two sequences of numbers are independent and random, the sum of the products will tend to zero as the number of pairs of points is increased to infinity, as all numbers positive and negative are equally likely. If however, the sum is finite and non-zero

this will indicate a degree of correlation. A negative result will occur if one sequence increases as the other decreases. Thus, the cross-correlation coefficient r between two data sequences I_1 and I_2 of equal length can be expressed as

$$r = \frac{1}{N}\sum_{n=1}^{N} I_1(n)I_2(n) \tag{3}$$

The $1/N$ term is included in the definition of the cross-correlation to insure that the result is independent of the number of sampled points. Unfortunately however, the value of the correlation coefficient will greatly depend upon the absolute values of the respective data sets. This can be overcome by normalising the coefficient to the range $-1 \leq r \leq 1$. This in turn can be accomplished by normalising the cross correlation coefficient by the factor

$$\sqrt{\left(\frac{1}{N}\sum_{n=1}^{N} I_1^2(n)\right)\cdot\left(\frac{1}{N}\sum_{n=1}^{N} I_2^2(n)\right)} = \frac{1}{N}\sqrt{\left(\sum_{n=1}^{N} I_1^2(n)\right)\cdot\left(\sum_{n=1}^{N} I_2^2(n)\right)} \tag{4}$$

Thus, the normalised correlation coefficient can be expressed as

$$r = \frac{\sum_{n=1}^{N} I_1(n)I_2(n)}{\sqrt{\left(\sum_{n=1}^{N} I_1^2(n)\right)/\left(\sum_{n=1}^{N} I_2^2(n)\right)}} \tag{5}$$

This is usually known as a cross-correlation coefficient and, as shown above, it is normalised so that its value always lies in the range $-1 \leq r \leq 1$, where $+1$ implies perfect correlation, 0 signifies no correlation and –1 represents opposite signals, i.e. signals out of phase by pi.

Figure 5 shows the correlation coefficients for the 99 angular error data sets where again the data points have been joined by a solid line for ease of observation.

4.2 Simulation of AUT-to-probe separation error

Range length errors were modelled in the same fashion as the angular errors. However, the maximum variation was determined from an error analysis of the fabrication and use of the AUT mechanical positioner. A further 99 measurement simulations were generated, transformed to the far field, and plotted. Cardinal cuts can be seen overlaid in Fig. 6.

Figure 6 appears to illustrate that the errors associated with the probe separation error are of limited angular extent, centred about angles that correspond to directions in which similar strength signals are combined from the different acquisition planes. Additionally, the error becomes smallest for angles that are derived primarily from the signal associated with a single scan. Inevitably, such interference effects are at wide angles where the overall signal strength is reduced.

Figure 7 again contains the perfect alignment result plotted with the maximum EMPL value at each of the angles from all 99 simulations. This clearly confirms that the greatest errors are observed over a limited wide-out angular range. Although raising the EMPL to perhaps as little as 10 dB below the error free signal at $\pm 60^\circ$, the auxiliary rotation system was again sufficiently resilient not to break down. Again, its failure is gradual, illustrating a degree of robustness that should be observed in practice.

Unfortunately, although the EMPL is useful for highlighting differences between patterns and measurement errors, it fails to deliver a single quantitative metric of similarity between patterns that can be used to determine which of these different phenomena is most important.

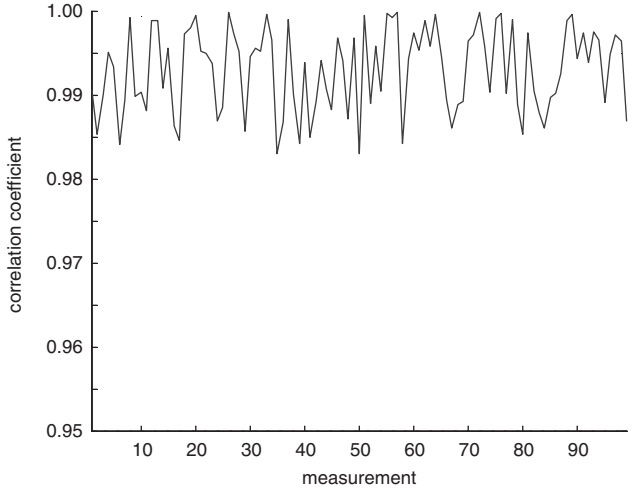

Fig. 5 *Correlations for the 99 angular errors*

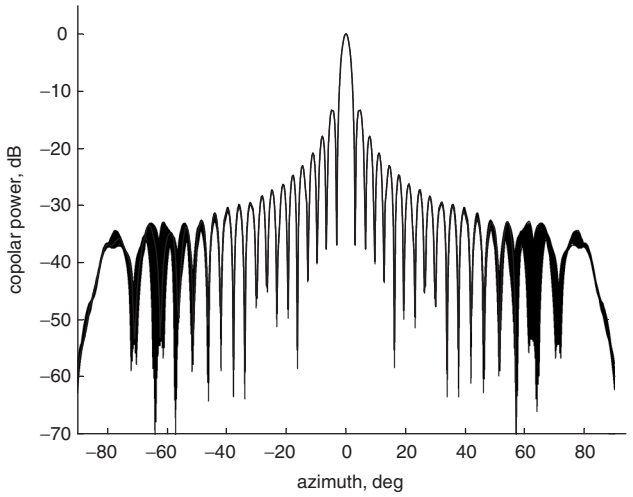

Fig. 6 *Far-field azimuth cut of all simulations*

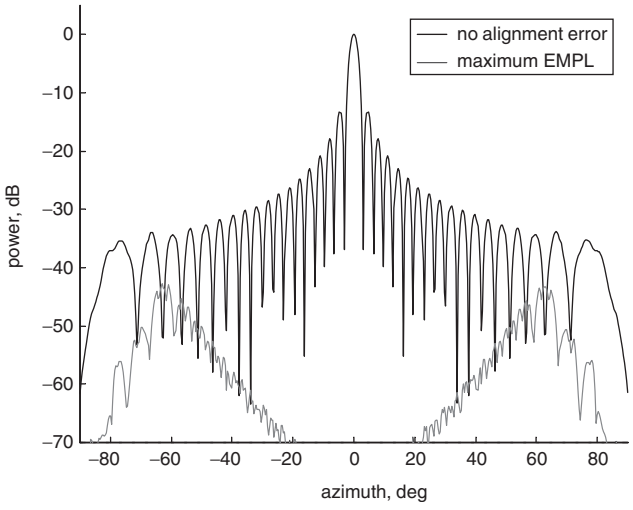

Fig. 7 *Far-field azimuth cut of ideal simulation and maximum EMPL*

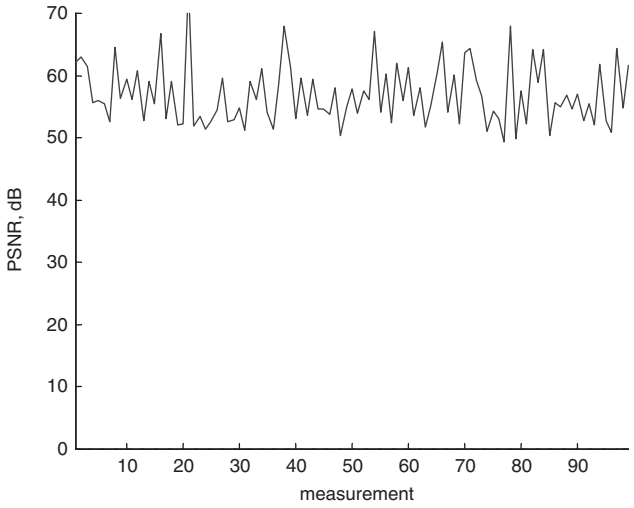

Fig. 8 *$PSNR_{dB}$ 99 down range errors*

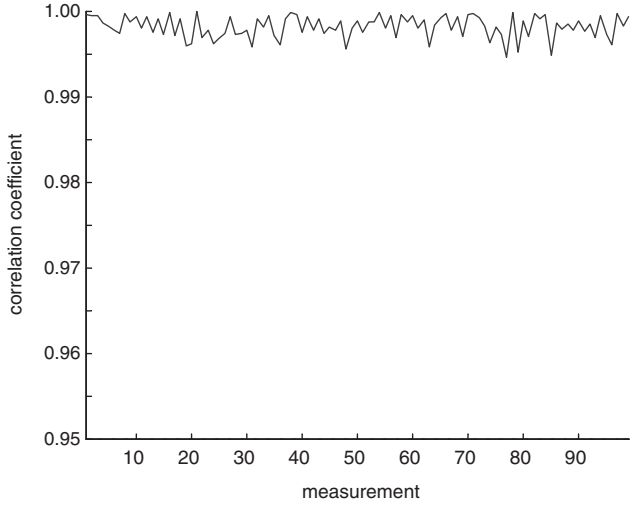

Fig. 9 *Correlations for 99 down range errors*

As for the angular errors, the $PSNR_{dB}$ and cross-correlation can also be calculated for the simulated down range error antenna patterns, and these are shown as Figs. 8 and 9.

4.3 Summary of conventional techniques

All of the above conventional techniques have advantages and limitations associated with them, primarily as they are all designed to produce comparisons of data sets that do not share the characteristics of antenna patterns.

The EMPL level is an easily evaluated metric that is conceptually simple as broadly, it represents the size of signal required to make the two different signals the same. Thus, this technique is highly sensitive to the presence of a constant displacement between the comparison data sets. However, if necessary, phase information can be taken into account by taking the difference between the respective complex voltages.

It is often used to represent the uncertainty associated with a given data set, i.e. analogous to an error bar. The principle limitation of this technique is that it fails to produce a single, or small number, of coefficients that can be used to describe the data set. Instead, it produces a value for each element in the comparison data sets. This not only results in the EMPL having to be presented graphically, but also requires that the comparison data sets should contain an equal number of elements, although this difficulty can often be resolved with the use of interpolation.

As this is a local interval assessment technique, the results are, often sensitive and discontinuous obscuring subtler underlying features. Such effects can be mitigated by smoothing, i.e. by taking a 'boxcar average', although this is undesirable as the fidelity of the response is compromised.

The PSNR is a measure often employed to assess the difference between two digital images. PSNR is the ratio of the largest signal to the arithmetic root mean square of the differences between the respective data sets, and as such the presence of a constant offset between data sets will dominate the value of the PSNR. For the case of antenna measurements, an accurate absolute reference can only be obtained by way of a gain calibration, which is difficult and often inaccurate.

Although the PSNR approach yields a single coefficient, it has the complication of having an infinite range, i.e. $0 \leq k \leq \infty$, when expressed in dB. In practice, this metric is found to be enormously sensitive with patterns that are essentially very similar yielding differences, as can be seen in Figs. 4 and 8, of as much as 20 dB. Although this technique is global i.e. it takes account of differences between every part of each data set it fails to take account of phase information and as it is a purely interval technique, it is sensitive to the influence of outlying points. Finally, the evaluation of the PSNR requires that the respective data sets contain the same number of elements.

The cross-correlation coefficient is a computationally expensive, general-purpose technique for obtaining a single quantitative, correctly normalised measure of adjacency; the technique is often used to calibrate time delays or offsets between theoretically identical signals. For the case of antennas, this would equate to determining the pointing error of a known antenna pattern function.

Again, it is a holistic metric although unlike the previous techniques, zero padding the smaller data set can accommodate data sets of differing sizes. The cross-correlation coefficient can take account of amplitude and phase data, provided that the data sets are represented in rectangular form. However, as it is a purely interval technique that essentially relies upon a summation process, it is both potentially numerically unstable and sensitive to the presence of outlying points. In practice, minor differences between otherwise similar patterns are not well discriminated, as for the case of the simulations presented above where the differences were mainly reported in the third decimal place.

5 Novel measures of correspondence

The measured and simulated data sets are complex and the integral transforms that are used on them are holistic. This suggests that assessment methods that are based on extracting features from the patterns that are universal to the entire pattern, as opposed to specific to localised areas, would be useful in the assessment process. Therefore, the identification of pattern features that are a function of the entire pattern that can then be analysed to calculate a measure of comparison or adjacency in the feature space are desirable.

5.1 Interval measures

A statistical interval measurement of correspondence based on calculating the moments of the antenna pattern when it is treated as a probability distribution has already been reported [2]. Moments of a probability density function describing area, centroid, variance, kurtosis and skewness

yield 15 numerical values that characterise the data. These calculated numerical values effectively dimensionally reduce the data set to 15 numbers which represent 15 global or universal features of the entire pattern.

Viewing these 15 variables in a fifteen dimensional feature space yields a vector, and comparison of two such vectors will enable comparison of the two data sets. The technique used here is to construct an orthogonal vector to the first data set and then take the dot product with the second to form the comparison. Here, if they are exactly the same the dot product will be zero. The vector's modulus and argument form the comparison of similarity between the two patterns. Figures 10 and 11 illustrate the calculated error vectors plotted on a feature plane from the interval moment assessment method, for the angular error and range length error simulations, respectively.

The central region of Fig. 10 aligns closely with that of Fig. 11, but the large values of EMPL associated with the angular errors extend the error points through the error vector space to produce a more extended trajectory through it. This is expected, as the error terms obtained during the range length analysis were located principally in regions of small field intensity. This trajectory appears to be related both to the extent of the angular nature of the errors, and to the shape of the underlying pattern.

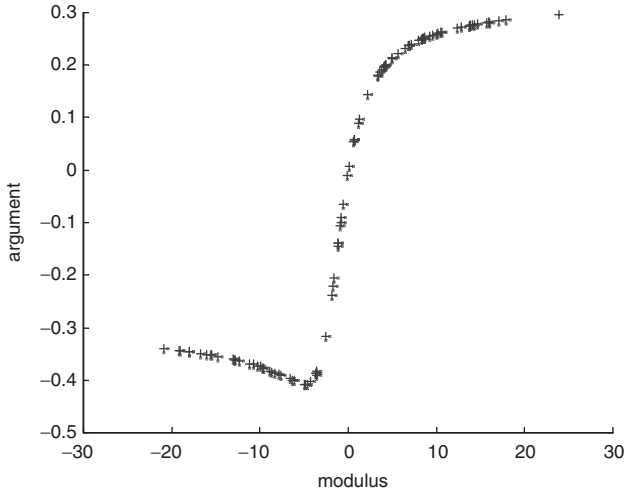

Fig. 10 *Feature plane plot of interval moment assessment method for angular errors*

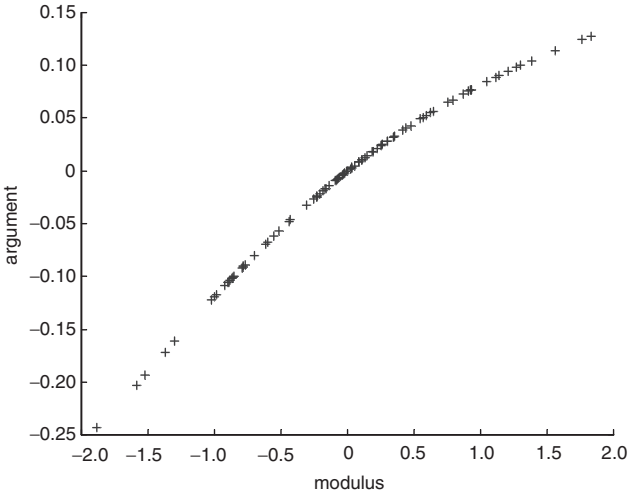

Fig. 11 *Feature plane plot of interval moment assessment method for range length errors*

In this methodology of comparison, all of the moments are given the same weight irrespective of the fact that they are calculated from a series of moments that are higher and higher powers of the co-ordinates of the data points in the angular pattern. If required, as with antenna measurements, the calculated moments can be normalised, with respect to the moments of the pattern of a gain standard, which can then be used to scale the calculated moments relative to the gain standard prior to comparison.

However, there are two specific aspects of the measurement methodology that handicap any interval pattern assessment of antenna patterns produced by near-field scanning:

- the very high dynamic range of the measurement system;
- the interferometric nature of the measurement and the lack of uniformity of the reference source.

Both of these mean that interval assessment of the data sets can lead to misleading results; as such, an interval methodology depends on absolute signal levels, while the measurement technique is based on relative interferometric test and reference signal level measurements.

5.2 Ordinal measures

An ordinal measure of association that overcomes this limitation can be derived if the interval nature of the data is ignored. If ranked in terms of the amplitude, all antenna data sets sampled over the same intervals and containing the same number of elements are bijections between the set and itself, i.e. permutations of the same elements [7]. The only possible variation is in where these elements are to be found in the data sets and therefore, the 2×99 data sets all represent different permutations of the same data. Thus, it is the similarity of the permutations that is assessed and by inference, also the data from which the permutations are constructed.

This provides the opportunity to construct a measure of association based on the inverse permutation of data sets with respect to each other. This will produce a metric of correspondence that is immune to many of the pathological inconsistencies of such large interval data sets.

Any proposed objective measure of correlation, or association, between data sets based on this methodology would be desired to be:

- a single coefficient, independent of scaling or shift due to the differences in reference levels,
- insensitive to the large dynamic range of the data,
- normalised, i.e. give correlation value ranging between –1 and 1, and finally,
- symmetrical or commutative to the operation of correspondence.

If we assume a suitable methodology for defining a single coefficient and normalising it between –1 and +1 can be found. As the range of values in the permutation is limited to the number of elements in the set, the dynamic range is also limited but not restrictive. Additionally, permutations mirror Abelian symmetry under a group operation [7], and therefore are by definition symmetrical and commutative. Thus, such a measure of association based on the correlation of the permutations derived from the data sets is possible.

Within the image processing community such a measure has already been devised and implemented [8] and it can be applied to the assessment of antenna patterns [3]. Following the development of [8], this measure is expressed in terms of a rank permutation which is obtained by sorting the data in ascending order and then labelling each element with integers accordingly, i.e. $[1, 2, 3, \ldots, n]$ where n is the number of elements in the set.

The correlation between two rankings can be considered to constitute a measure of closeness, or distance. For a set of amplitude values I_1 and I_2, let π_1 be the rank of element I_1^i among I_1 and π_2 be the rank of element I_2^i among I_2. If the ranks are not unique, i.e. two elements have the same value, then the elements are ranked so that the relative spatial ordering between elements is preserved. A composition permutation s is defined such that s^i is the rank of the element in I_2 that corresponds to the element with rank π_1^i in I_1. Hence, for the case of a perfect positive correlation, $s = (1, 2, 3, \ldots, n)$, where n is the number of elements in the set.

The definition of a distance metric to assess the distance between s and the identity permutation $u = (1, 2, 3, \ldots, n)$ will result in a measure of the distance between π_1 and π_2. The distance vector d_m^i at each s^i is defined as the number of s^j where $j = 1, 2, 3, \ldots, i$ which are greater than i. This can be expressed as

$$d_m^i = \sum_{j=1}^{i} J(s^j > i) \tag{6}$$

where $J(B)$ in an indicator function which is defined as

$$J(B) = \begin{cases} 1 & \text{when } B \text{ true} \\ 0 & \text{when } B \text{ false} \end{cases} \tag{7}$$

Here, d_m^i can be thought of as a measure of the number and the extent to which the elements are out of order. If I_1 and I_2 were perfectly correlated, then the distance measure will become a vector of zeros, i.e.

$$d_m(s, u) = (0, 0, 0, \ldots, 0) \tag{8}$$

Several examples of this process can be found in the Appendix. The maximum value that any component of this distance vector can take is $n/2$, which occurs for the case of a perfect negative correlation. Finally, a coefficient of correlation can be obtained from the vector of distance measures as

$$k(I_1, I_2) = 1 - \frac{2 \max_{i=1}^{n} d_m^i}{n/2} \tag{9}$$

Here, if I_1 and I_2 are perfectly correlated, then $(s = u)$ and $k = 1$. When I_1 and I_2 are perfectly negatively correlated, then $k = -1$.

The ordinal coefficient of correlation k was computed between the reference data set and each of the results from the error simulation contained in Figs. 2 and 3. Each of these 99 coefficients can be found as the solid line in Fig. 12. For the sake of clarity, the discrete k values are presented in terms of a line graph. Table 1 contains the mean value, median value, standard deviation and 99% confidence interval for the range of k values obtained for the angular error simulations.

This operation was repeated for the simulations based upon range length errors. The ordinal coefficient of correlation k was computed and the results can be found presented as the solid line in Fig. 13. The mean value, median value, standard deviation and 99% confidence interval for the ranges of k values obtained are shown in Table 2.

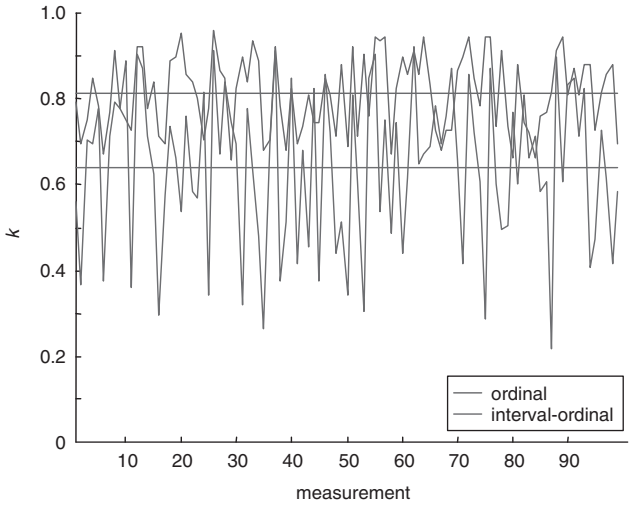

Fig. 12 *Plot of ordinal k and modified interval-ordinal k as a function of simulation for angular errors*

Table 1: *k* values for azimuth cut of angular error simulations

Metric	*k*
Mean	0.8132
Median	0.8160
Standard deviation, σ	0.0879
3σ (99% confidence level)	0.2638

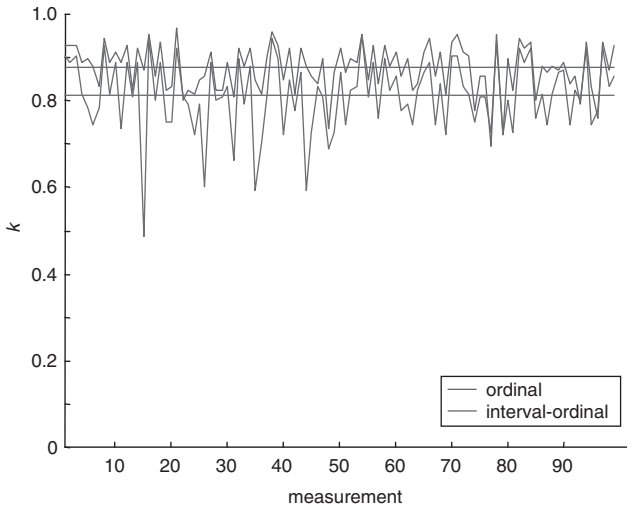

Fig. 13 *Plot of ordinal k and modified interval-ordinal k as a function of simulation for range length errors*

Table 2: *k* values for azimuth cut of range length error simulations

Metric	*k*
Mean	0.8758
Median	0.8800
Standard deviation, σ	0.0546
3σ (99% confidence level)	0.1638

The results of the ordinal measure clearly show that the small but systematic errors introduced into the simulations can be accurately quantified in the calculation of the k value. However, from Figs. 2 and 3 it is clear that the angular distribution of errors is independent of far-field angle for the angular error case whilst it is correlated to specific far-field angles for the range length case, cf. Figs. 6 and 7.

The ordinal process of ranking the data to produce permutations takes no account of either the absolute amplitude or spatial angles at which the data is found; thus, every region of the pattern is judged to be equally important in the calculation of k. This is clearly illustrated by comparison of the mean average values of k determined from the two different error simulations.

To differentiate between errors that are not uniformly located across the data sets some method of isolating the effects of these localised errors must be established. In Fig. 7 the maximum EMPL is located around specific angles relative to boresight and seems to be at distinguishable amplitudes relative to boresight. Therefore, any process that distinguishes between areas in the pattern in terms of spatial angle or relative amplitude could be used to modify the data prior to ranking, so that the resultant permutations would be biased to reflect these localised areas in the patterns.

By inspection of Fig. 7 it is clear that the differences observed equate to lower signal levels than those in Fig. 3. However, this is not reflected by a significant difference in their respective k values.

5.3 Ordinal interval (hybrid measures)

The ordinal measure of association can be readily modified to take account of different regions of interest by re-tabulating the data in such a way as to attribute more samples to regions of greatest interest prior to ranking the data. This approach minimises the impact of numerical instabilities as observed when using a purely interval assessment technique, but produces a permutation that is weighted to take more account of the specific property of the patterns that is judged to be important, i.e. higher signal levels.

Assuming that the patterns are sufficiently well sampled, this can readily be determined for the case of antenna radiation patterns. Such a re-tabulation can be accomplished rigorously through the application of the sampling theorem i.e. Whittaker interpolation. Alternatively, this can be performed efficiently albeit with approximation, using piecewise polynomial functions, i.e. cubic spline or cubic convolution interpolation.

The solid trace in Fig. 12 contains results from calculations of the k value pertaining to the angular error simulation. The dotted trace represents the k values obtained from the hybrid ordinalinterval technique where the data was re-tabulated so that more samples were attributed to regions of larger field intensity.

Figure 13 contains similar data obtained from the range length error simulation. This illustrates that the hybrid technique is better able to isolate errors in the data sets that display amplitude specific traits. The mean hybrid coefficient k for the angular error simulation was 0.6395 whereas that obtained from the range length simulation was 0.8113, reflecting the greater impact of angular errors in regions of higher field strengths around boresight.

From the Figures, it can clearly be seen that the extent to which the hybrid interval-ordinal method discriminates between differences in elements corresponding to signal magnitudes can be readily varied on a case-by-case basis, to emphasise or de-emphasise the particular feature under investigation.

The ordinal and hybrid interval-ordinal methodologies both overcome many of the disadvantages displayed in traditional and novel interval assessment strategies but they do place constraints on the types of data sets that can be compared. The comparison of permutations requires the two data sets to be, either identical in terms of sampling interval, extent and number of data points, or for it to be possible to interpolate the sets to arrive at a situation where these conditions hold. For complex multidimensional data sets containing many different angles and frequencies this is often impossible.

5.4 Categorical ordinal (hybrid measures)

Some of these difficulties can be overcome and different data set structures can be compared if, prior to the ordinal assessment, the data sets are categorised and then the relative frequencies associated with the categorisation are the subject of the ordinal measure of correspondence.

Although there are a great many ways of categorising a given data set, one of the simplest is to divide the interval data set into a number of amplitude bins and to count how many elements fall within each bin, i.e. a categorical interval methodology. Each data set that is compared will provide a single histogram that can be normalised before subsequently being processed to provide the measure of correspondence. Normalisation would usually be accomplished by ensuring the total summation of the frequencies of the two sets to be compared was equal while the relative frequencies for the bins in each data set remained constant.

The level and size of the bins can be arbitrarily chosen. This enables a preference to be made as to what is to be emphasised, i.e. the bins can be distributed in a non-linear fashion. Thus, more bins can be used for large signals than for small signals or *vice-versa*. In the limit, when the bins are sufficiently small and sufficiently numerous, their will be one bin per distinguishable amplitude. For double-precision arithmetics the floating-point accuracy is approximately 10^{-12}. Figures 14 and 15 contain the histograms obtained from two typical far-field pattern functions when expressed linearly.

As is clear from these Figures, the histograms are poorly distributed with most of the samples occupying only a small number of bins. Clustering such as this can be resolved by redistributing the bins. Figures 16 and 17 contain

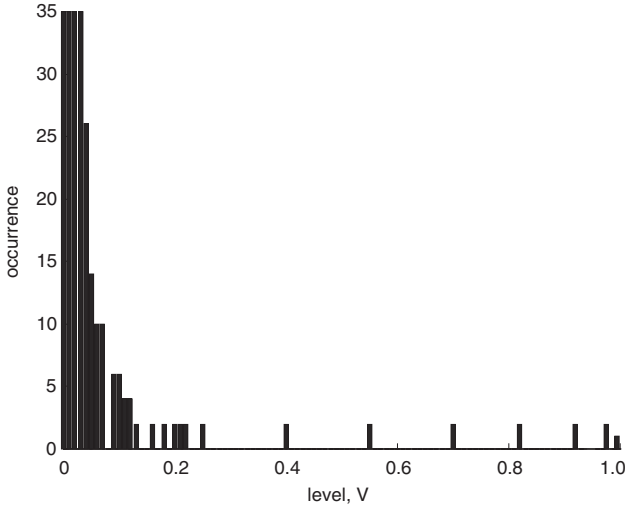

Fig. 14 *Histogram of two-dimensional reference pattern function (reference data set)*

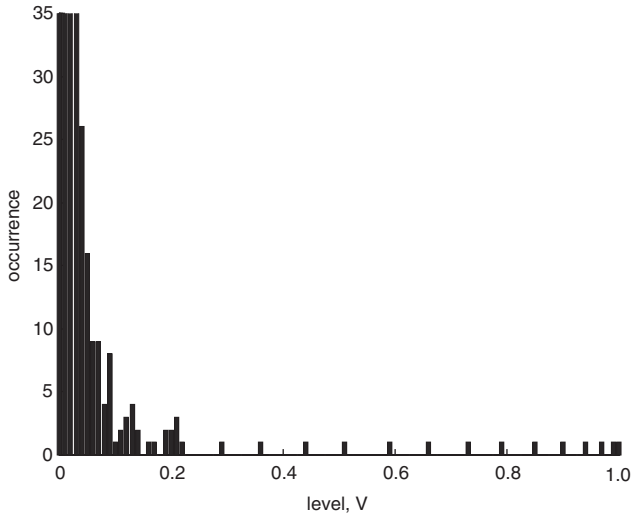

Fig. 15 *Histogram of two-dimensional reference pattern function (comparison data set)*

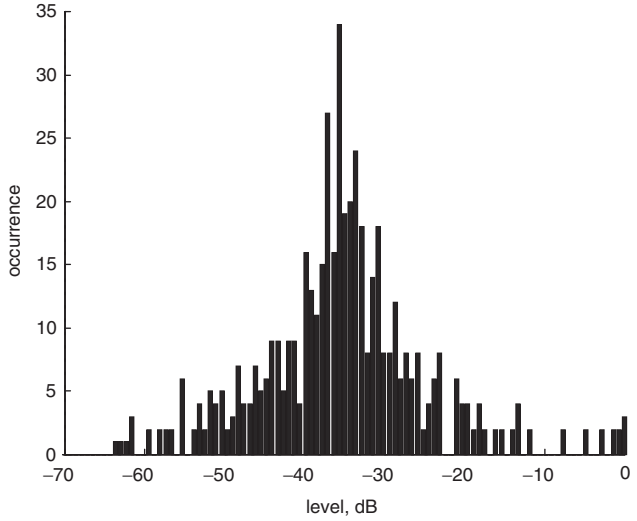

Fig. 16 *Histogram of two-dimensional reference pattern function (reference data set)*

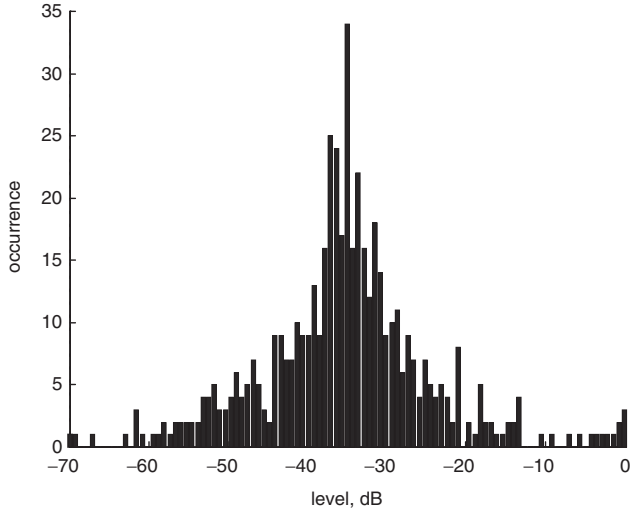

Fig. 17 *Histogram of two-dimensional reference pattern function (comparison data set)*

histograms from the same data sets. However, the bins have been chosen so that they are linearly distributed on a logarithmic scale. Here, the interval data set has been divided into 101 bins that spanned from –70 dB to 0 dB. The spread of these histograms can be readily increased by narrowing the interval of the bins, and/or increasing the number of bins used.

This categorical process yields a histogram vector of 101 elements that can be readily compared with another vector using the ordinal measure of adjacency detailed above. For these data, sets the ordinal measure of association k was 0.44.

6 Summary of novel techniques

The interval statistical image classification technique is highly sensitive which in part results from the huge dynamic range inherent in the data, and in part from the use of large, i.e. up to fourth order, statistical moments. Unfortunately, although the technique is holistic it yields two values per comparison and is particularly sensitive to the influence of outlying points. Furthermore, pronounced differences between patterns can result in numerical instabilities resulting in the two co-ordinates of the feature plane differing by more than six orders of magnitude. Such numerical instabilities can in part be resolved by normalising the moments with respect to a calibration standard, i.e. reference antenna, whereby each of the moment vector components becomes equally important. On the positive side of the balance sheet, statistical image classification can be embodied within a very efficient algorithm that is easily evaluated on a digital computer.

The ordinal measure of association yields a single quantitative, normalised coefficient that has in practice been found to be extremely robust. However such robustness tends to render the technique insensitive to smaller differences, particularly to 'textures' within the pattern, i.e. to subtitles within the overall pattern.

Unlike its interval counterpart, the calculations required to determine the coefficient k are somewhat lengthy, even for relatively small data sets. As this technique relies purely upon the order of the elements within the respective data sets, differences between large signals are as equally important as similar differences between small signals, and in practice, this can render the technique sensitive to the presence of noise.

The hybrid technique takes account of the interval aspects of the data set by apportioning a greater number of samples to regions of greatest interest whereupon the modified data sets are compared using the ordinal measure of association discussed above. For example, this re-tabulation process enables the influence of low-level noise to be suppressed, i.e. the presence of large differences between small signals on essentially identical data sets to be suppressed, whilst retaining all of the advantages of the interval assessment technique.

It therefore allows more detailed characterisation and classification of specific error sources in the measurements, allowing the interval nature of the data to influence the ordinal permutations that are abstracted from the data. Furthermore, the technique can similarly be extended to take greater account of data occupying particular angular regions of space. Thus, the comparison process can be tailored to characterise specific error sources in the measured data sets and to assess their importance.

The principle advantage of categorisation prior to processing with the standard hybrid interval-ordinal technique, lies within the fact that a histogram can be

made of data sets that contain different number of elements. Additionally it is automatically able to compare two-, three- or higher-dimensional data sets. Furthermore, as the comparison technique is often complicated by the large amounts of data present within the respective data sets, as the histograms can be made to be of arbitrary size, the efficiency of the comparison process can be greatly improved.

However, as the technique essentially compares two histograms, any ambiguity within the histogram representation of the data set will constitute an ambiguity in the correlation process. One potential weakness can be illustrated by examining the histograms obtained from the patterns contained in Fig. 18.

Figure 18 contains two traces that represent essentially the same data sets, only the order in which the elements are stored has changed, i.e. they are permutations of each other and could be effectively assessed via the ordinal or interval ordinal technique. However, as the values contained within the elements of set 1 and set 2 are identical, the histograms formed from these respective data sets will also be identical, as shown in Fig. 19.

As pattern functions 1 and 2 contain the same data the resulting histograms will be essentially identical, i.e. all of the elements of the histogram of set 1 will be the same as all of the elements of set 2 and thus

$$[h_1] - [h_2] = [0]$$

This insensitivity to direction is both the principle weakness of the histogram technique and consequently, the principle weakness of any comparison technique based upon it. The impact of such insensitivity will depend primarily upon the characteristics of the patterns being compared. However, a hybrid approach combining correlation and ordinal techniques offers promise here.

The principal differences between the various non-local distance metrics can be found summarised in Table 3.

7 Discussion and conclusions

Two principle sources of error within 'auxiliary rotation partial scan near-field measurement systems' have been modelled. The effects of these errors on the far-field vector pattern functions have been analysed using conventional metrics of determining measurement repeatability, and their shortcomings have been noted.

The far-field patterns have then been reassessed using three existing statistical techniques that consider the interval, ordinal and categorical aspects of the data. An interval technique based on the calculation of the moments of the data set, an ordinal and a new hybrid technique have been presented that extends to the ordinal technique an ability to differentiate specific distributed features in the data sets. The addition of a prior categorisation step has also been illustrated.

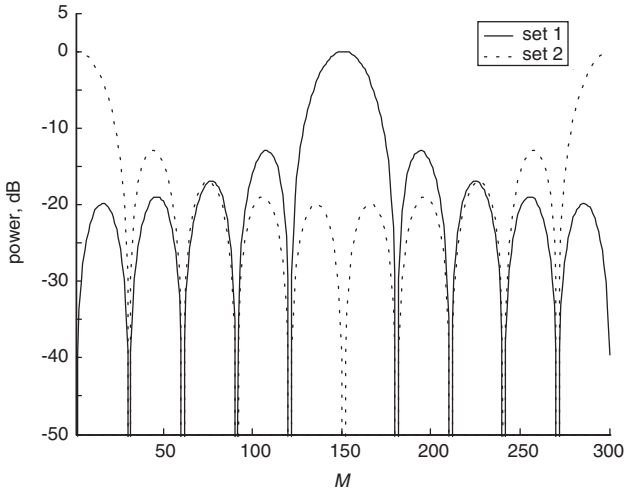

Fig. 18 *Pattern functions 1 and 2*

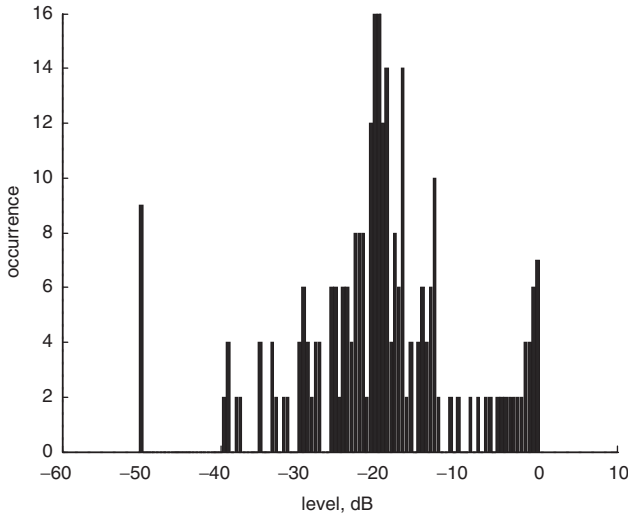

Fig. 19 *Histogram of pattern function 1*

Table 3: Qualitative comparison of various pattern comparison techniques

Metric	Interval	Ordinal	Single coefficient	Domain	Holistic	Robust	Sensitivity to outlying points	Absolute ref
Cross-correlation	yes	no	yes	$-1 \leq k \leq 1$	yes	no	yes	yes
Statistical moments	yes	no	no	N/A	yes	no	no	yes
Ordinal	no	yes	yes	$-1 \leq k \leq 1$	yes	very stable	no	no
Interval-ordinal	yes	yes	yes	$-1 \leq k \leq 1$	yes	stable	no	yes
Categorical-interval	yes	yes	yes	$-1 \leq k \leq 1$	yes	no	yes	yes
Categorical-ordinal	yes	yes	yes	$-1 \leq k \leq 1$	yes	very stable	no	yes

In the text, the comparison was made between the histograms, rather than between the respective data sets, by utilising the ordinal coefficient of correlation. However, the choice of method for determining the adjacency of the histograms is arbitrary and any of the comparison techniques discussed above could be utilised on the histograms of the data sets as well as on the actual data sets. Thus, after categorisation it is possible to provide categorical interval as well as categorical ordinal measures of correspondence.

All of the conventional and novel comparison techniques have particular areas of applicability where their specific characteristics are suited to the abstraction of the large data sets to distil their important or relevant features so that these can be quantitatively assessed. However, two of these techniques deserve a special note. The EMPL has been found to be particularly useful for graphically illustrating the differences between two one-dimensional pattern cuts whilst the ordinal measure of association has been found to be particularly adept at describing differences between two-dimensional pattern functions.

In principle, the hybrid ordinal-interval technique should offer significant advantages over the ordinal technique. However, at this time, it is not sufficiently mature for general purpose, unguarded use.

The research reported in this paper into antenna pattern measurement is ongoing and its extension to comparisons based on treating the data categorically in terms that are not interval value based is underway. However, it is clear that the new and novel antenna measurement techniques being pioneered at present offer an assessment challenge if the large volumes of data these techniques generate are to be quantitatively, effectively and concisely analysed and summarised.

8 References

1 McCormick, J., and Da silva, E.: 'The use of an auxiliary translation system in near field antenna measurements'. Proc. Int. Conf. on Antennas and Propagation, April 1997, Edinburgh, UK,Vol. 1, p. 190
2 Gregson, S.F., and McCormick, J.: 'Image classification as applied to the holographic analysis of mis-aligned antennas'. Presented at ESA ESTEC, 1999
3 Gregson, S.F., McCormick, J., and Parini, C.G.: 'Measuring wide angle antenna performance using small planar scanners'. Proc. IEE ICAP 2001, Manchester, UK, Apr. 2001
4 Feynman, R.P.: 'The Feynman lectures on physics' (Addison Wesley, CA, USA, 1964), Vol. 2, Chap. 28, pp. 28.1–28.10
5 Gregson, S.F., McCormick, J., and Parini, C.G.: 'Poly-planar near field antenna measurements'. Presented at IEE Antenna Measurement and SAR Technical Seminar, Loughborough, UK, 28–29 May 2002
6 Squires, G.L.: 'Practical Physics' (Cambridge University Press, Cambridge, UK, 2001, 4th edn.), pp. 9–16
7 Stewart, I.S.: 'Concepts of modern mathematics' (Dover Publications Ltd., 1995), pp. 100–109
8 Bhat, D.N., and Nayar, S.K.: 'Ordinal measures for visual correspondence'. Technical Report CUCS-009-96, Columbia University Centre for Research in Intelligent Systems, 1996

9 Appendix: Examples of the ordinal measure process

Example 1: Partial positive correlation: Consider the two data sets I_1 and I_2 where,

$$I_1 = [10, 20, 30, 40, 60, 50]$$

and

$$I_2 = [10, 20, 30, 40, 50, 60]$$

Let the rank of I_1 and I_2 be π_1 and π_2 respectively. Clearly

$$\pi_1 = [1, 2, 3, 4, 6, 5]$$

and

$$\pi_2 = [1, 2, 3, 4, 5, 6]$$

Now, $\boldsymbol{s}$ is a composition permutation. To find the first element of $\boldsymbol{s}$, search through the elements of π_1 to find the element containing the value 1 and make a note of its index. We use the value of the element of π_2 with the index corresponding to the index of the element already found in π_1 as the value of the first element of $\boldsymbol{s}$. This is then repeated for each element in $\boldsymbol{s}$. So consider finding the first element of $\boldsymbol{s}$, here, the first element in π_1 is equal to 1. So take the first element in π_2 and place it in the first element of $\boldsymbol{s}$. Now consider trying to find the 5th element of $\boldsymbol{s}$ for example. So, here the 6th element of π_1 is equal to 5. Now the 6th element of π_2 contains the value 6 thus the 5th element of $\boldsymbol{s}$ contains the value 6.

Repeating this procedure for each of the elements of s in turn yields:

$$s = [1, 2, 3, 4, 6, 5]$$

d_m^i is a distance vector where the value of the ith element of d_m^i depends upon the sum of a function that counts the number of out-of-order elements. This function contains the number of concurrent out-of-order elements, i.e. if one element is out-of-order the function takes the value 1, if two elements are next to one another and out-of-order the function takes the value 2 etc. Thus, as s contains only one out-of-order element then

$$d_m^i = [0, 0, 0, 0, 1, 0]$$

Since the maximum value of d_m^i is 1 then the coefficient of correlation is

$$K(I_1, I_2) = 1 - \frac{2 \times 1}{6/2} = \frac{1}{3}$$

Several more examples are presented below with just the results shown.

Example 2: Perfect negative correlation: Let, $\pi_1 = [6, 5, 4, 3, 2, 1]$ and $\pi_2 = [1, 2, 3, 4, 5, 6]$. Then

$$s = [6, 5, 4, 3, 2, 1]$$

Hence

$$d_m^i = [1, 2, 3, 2, 1, 0]$$

Thus

$$K(I_1, I_2) = 1 - \frac{2 \times 3}{6/2} = -1$$

Example 3: Partial negative correlation: Let, $\pi_1 = [1, 2, 6, 5, 4, 3]$ and $\pi_2 = [1, 2, 3, 4, 5, 6]$. Then

$$s = [1, 2, 6, 5, 4, 3]$$

Hence

$$d_m^i = [0, 0, 1, 2, 1, 0]$$

Thus

$$K(I_1, I_2) = 1 - \frac{2 \times 2}{6/2} = -\frac{1}{3}$$

Example 4: Insensitivity to texture: Let, $\pi_1 = [1, 3, 2, 4, 6, 5]$ and $\pi_2 = [1, 2, 3, 4, 5, 6]$. Then

$$s = [1, 3, 2, 4, 6, 5]$$

Hence

$$d_m^i = [0, 1, 0, 0, 1, 0]$$

Thus

$$K(I_1, I_2) = 1 - \frac{2 \times 1}{6/2} = \frac{1}{3}$$

Here we obtain the same coefficient of correlation as we did for the case when $\pi_1 = [1, 2, 3, 4, 6, 5]$ and $\pi_2 = [1, 2, 3, 4, 5, 6]$ although clearly there are more out-of-order elements, i.e. two, in this case. Such an occurrence is an example of insensitivity to 'texture' within a data set. Although this is clearly a disadvantage, it is not thought to be of primary importance when considering antenna radiation patterns.